

Geological Interpretation of Airborne Radiometric Data for Mineral Exploration Potential

*¹Ohaegbuchu, H. E., ²Ndubueze, D. N., ³Obiajulu, O. O. and ⁴Ahamefule, Y. C.



¹Department of Physics, Michael Okpara University of Agriculture, Umudike, Abia State

²Department of Physics, Kingsley Ozumba Mbadiwe University, Ideato, Imo State

³Department of Physics and Industrial Physics, Nnamdi Azikiwe University, Awka, Anambra State

⁴Department of Physics, Gregory University, Uturu, Abia State.

*Corresponding Author's Email: eo.henry@mouau.edu.ng Phone: +2348132954367

ABSTRACT

This study interprets airborne radiometric data to evaluate mineral exploration potential within a basement complex terrain. Concentration maps of potassium (K), thorium (Th), and uranium (U), together with ternary composites, radiometric ratios, and the Efimov F-parameter, were used to delineate lithological units and hydrothermal alteration zones. Elevated K values exceeding 1.2% occur mainly in the southeastern and central regions, accompanied by high K/Th ratios (>0.09) and positive F-parameter anomalies (>0.2), indicating potassic alteration. Uranium highs exceeding 6 ppm and elevated U/Th ratios (>0.3) mark zones of uranium mobility and secondary enrichment. The integration of all radiometric products highlights extensive hydrothermal alteration in the southeastern and central sectors, which is spatially associated with structural trends typical of orogenic mineral systems. Comparison with earlier radiometric studies across Nigeria, Morocco, Egypt, and Senegal confirms the reliability of these indicators. The identified zones represent high-priority targets for gold and base-metal exploration.

Keywords:

Airborne radiometrics,
Hydrothermal alteration,
Potassium,
Thorium,
Uranium,
Mineral exploration,
F-parameter.

INTRODUCTION

Airborne gamma-ray spectrometry provides a rapid and effective method for mapping the distribution of natural radioactive elements—potassium (K), thorium (Th), and uranium (U)—within the upper weathered zone of the Earth's surface. Because these elements exhibit predictable geochemical behaviours during metamorphism, magmatism, and hydrothermal alteration, radiometric data are widely used to discriminate lithologies and identify alteration zones associated with mineralization.

Applications in basement terrains have been demonstrated in numerous studies. Akinlalu (2023) identified potassic alteration related to gold mineralization in southwestern Nigeria using airborne radiometrics. Faruwa et al. (2021) showed that combined magnetic–radiometric interpretation improves recognition of litho-structural settings favourable for mineralization. Comparable methods have been applied

in Senegal (Thiam et al., 2023), Egypt (Kotb et al., 2024), and Morocco (Mamouch et al., 2022), underscoring the role of radiometrics in mapping alteration and lithological variability.

This study applies integrated radiometric techniques—including K, Th, U concentrations; ternary imaging; ratio maps; and the Efimov F-parameter—to delineate lithological units and identify hydrothermal alteration zones in a typical basement complex terrain.

Geological Setting

The study area comprises Precambrian crystalline basement rocks including migmatites, banded gneisses, schists, quartzites, and granitic intrusions (Figure 1). These units form part of the Pan-African basement of Nigeria, characterized by NE–SW structural trends produced during the Pan-African orogeny (Ohaegbuchu et al., 2025).

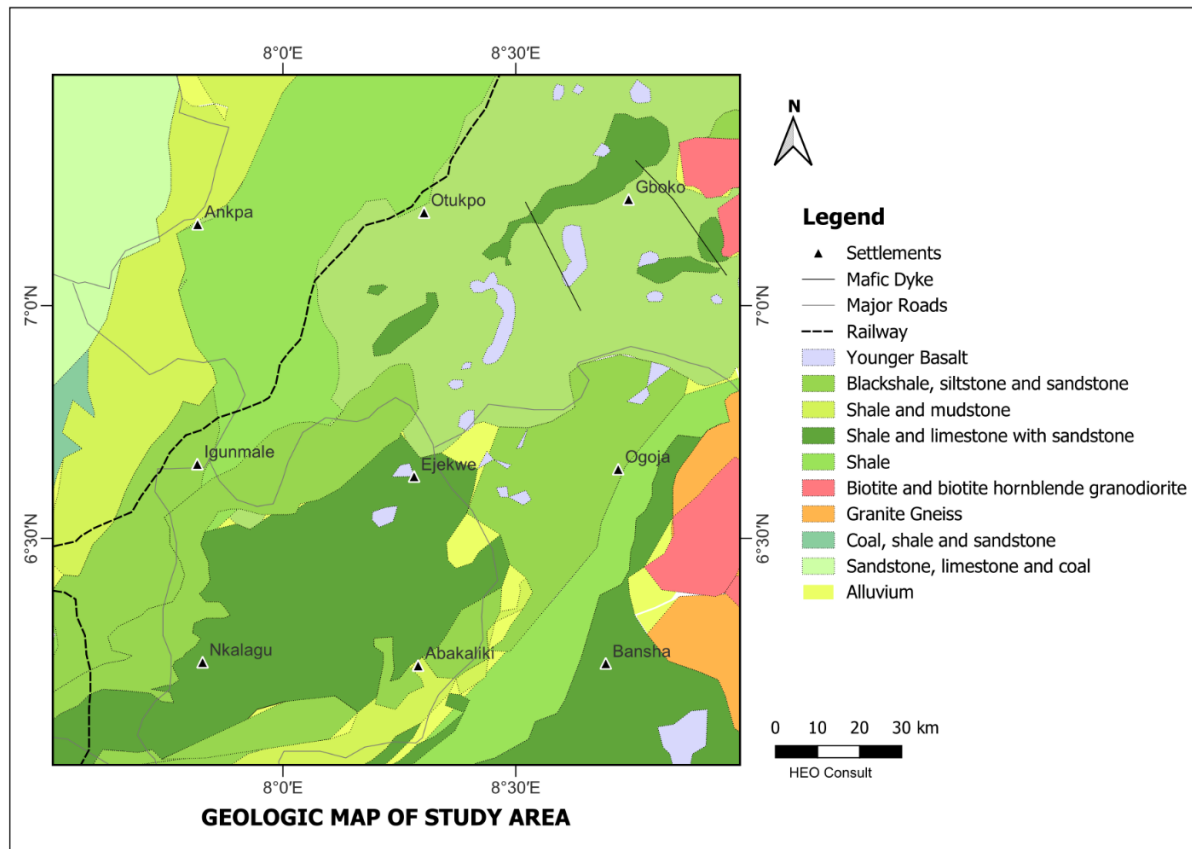


Figure 1: Geologic map of the study area showing the distribution of major lithological units and structural features. Granitic intrusions, migmatites, gneisses, and schistose units are identified alongside the dominant NE–SW and NW–SE structural trends that serve as fluid conduits and control the spatial arrangement of alteration zones highlighted by the radiometric survey.

Structures such as shear zones and fracture systems play a fundamental role in fluid migration and mineralization. Adegbuyi et al. (2021) demonstrated the importance of structural orientation and deformation fabrics in controlling mineralized zones across the Nigerian Basement Complex. The lithological diversity and strong structural imprint provide a favourable environment for hydrothermal alteration detectable by radiometric methods.

MATERIALS AND METHODS

Data Processing

Airborne gamma-ray spectrometric data were corrected for background, aircraft altitude, radon, and Compton scattering. Elemental concentrations were computed from count rates using:

$$X = S_X (C_X - B_X) \quad (1)$$

where X represents the concentration of K (%), Th (ppm), or U (ppm), S_X is the sensitivity coefficient, C_X the measured count rate, and B_X the background correction. These standardized procedures ensure reliable concentration values (Youssef, 2013).

Radiometric Ratios

Radiometric ratios improve recognition of alteration because Th is relatively immobile, whereas K and U are mobile during metasomatism.

Potassium–Thorium Ratio

$$K/Th = \frac{K(\%)}{Th(\text{ppm})} \quad (2)$$

High K/Th values indicate potassic enrichment (Shives, 2000).

Uranium–Thorium Ratio

$$U/Th = \frac{U(\text{ppm})}{Th(\text{ppm})} \quad (3)$$

Elevated U/Th values highlight uranium mobilization (Ohwo & Soalpe, 2024).

Ternary Radiometric Image

A ternary composite was generated, assigning red to K, green to Th, and blue to U. This enhances lithological contrasts and highlights multi-element anomalies (Mamouch et al., 2022).

Efimov F-Parameter

Efimov's alteration parameter detects thorium depletion relative to K and U:

$$F = \frac{(K \times U)}{Th} \quad (4)$$

High positive values indicate thorium-depleted altered zones (Kotb et al., 2024).

Interpretation Strategy

Interpretation integrates elemental concentration maps, ratio maps (K/Th and U/Th), ternary composites, and the

F-parameter distribution. This multi-parameter approach aligns with best practices described by Thiam et al. (2023) and Faruwa et al. (2021).

RESULTS AND DISCUSSION**Potassium (K) Distribution**

Potassium values range from less than 1% to more than 1.2% (Figure 2). The southeastern and central parts contain K concentrations exceeding 1.16%, suggesting potassic granitoids or hydrothermal K-metasomatism.

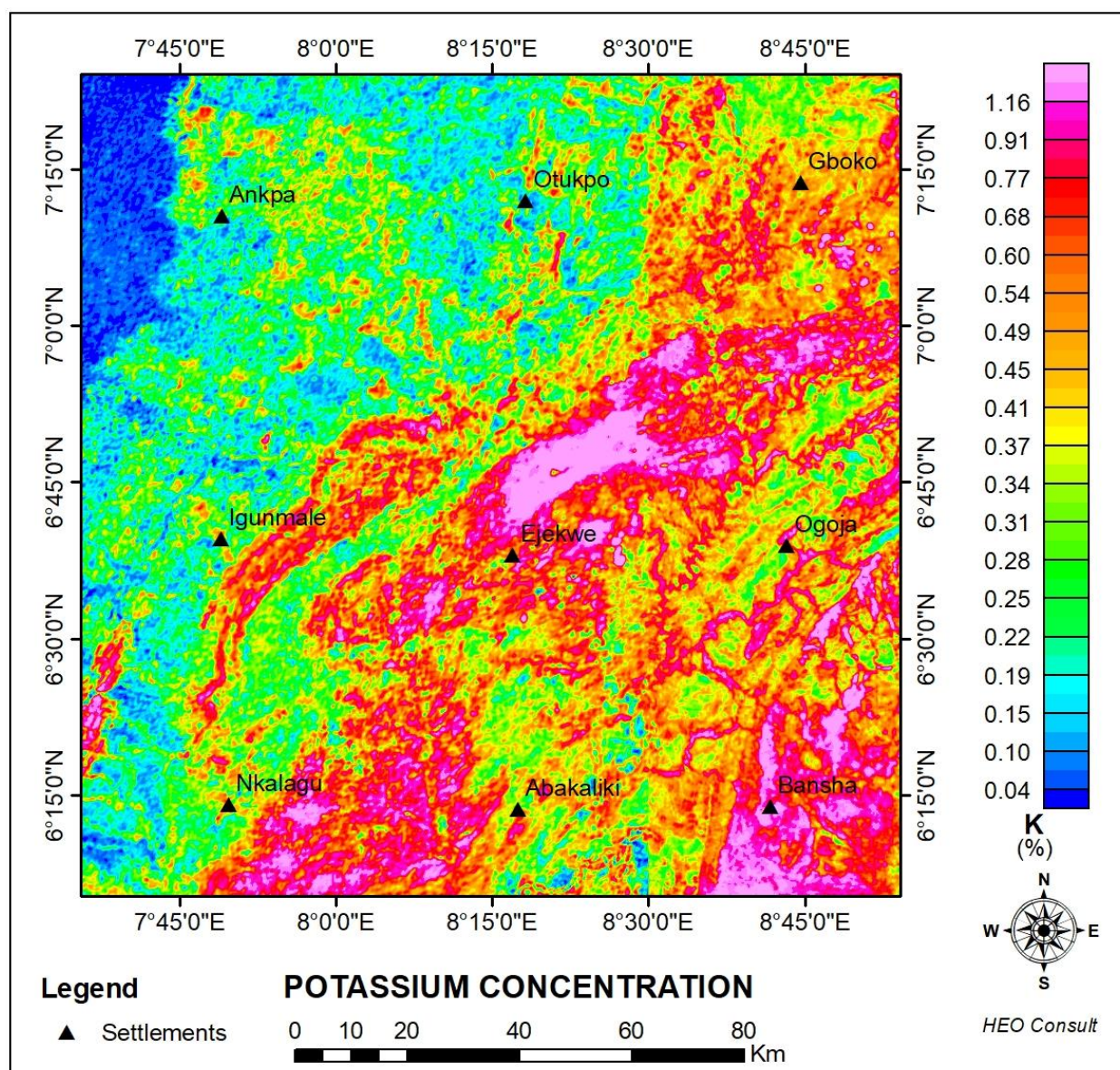


Figure 2: Potassium concentration map derived from the airborne γ -ray spectrometric dataset. Areas of elevated K reflect felsic lithologies and zones of potassic alteration, commonly linked to hydrothermal processes. High-K domains coincide with structural intersections and granitoid bodies, indicating potential pathways for mineralization.

Lower K values (<0.4%) in the northwest likely correspond to mafic or intermediate rocks or K-depleted alteration. These patterns are consistent with Shives (2000), who associated high K signatures with potassic alteration in mineralized terrains.

Thorium (Th) Distribution

Thorium ranges from approximately 4 ppm to over 20 ppm (Figure 3). High Th values (>15 ppm) in the northwest and central regions reflect felsic intrusions or pegmatites.

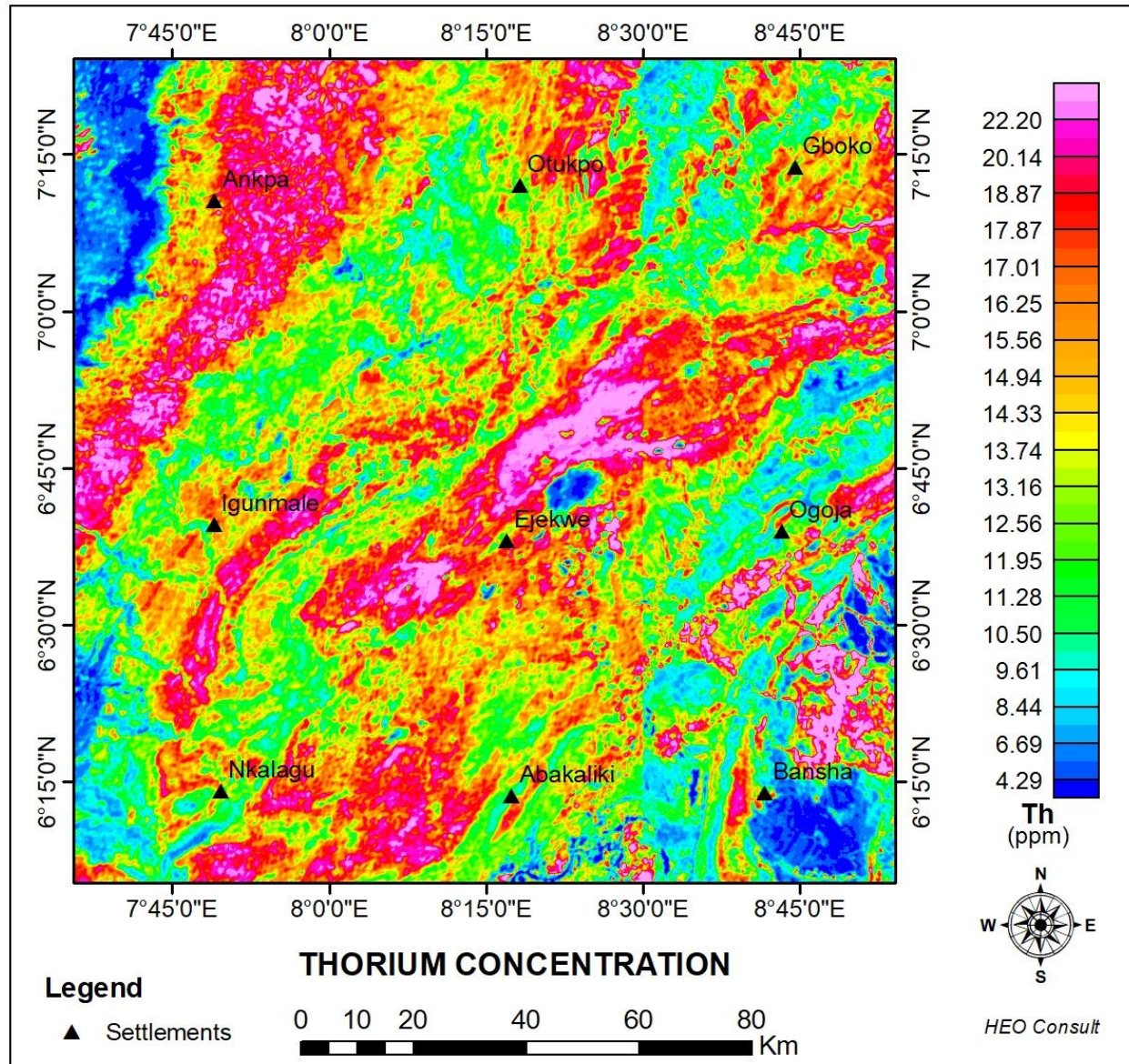


Figure 3: Thorium concentration map showing the distribution of eTh across the study area. Thorium, being relatively immobile during hydrothermal alteration, provides a stable lithological background. Zones of reduced eTh, especially where they coincide with elevated K, support the presence of potassic metasomatism and altered felsic units.

Low Th values (<14 ppm) in the southeastern region align with mafic or intermediate lithologies. Because Th is immobile, its distribution mainly reflects primary lithology (Xu, 2022; Liao et al., 2023).

Uranium (U) Distribution

Uranium varies from less than 2 ppm to more than 6 ppm (Figure 4). Significant anomalies exceeding 5 ppm are present in the northwestern zone.

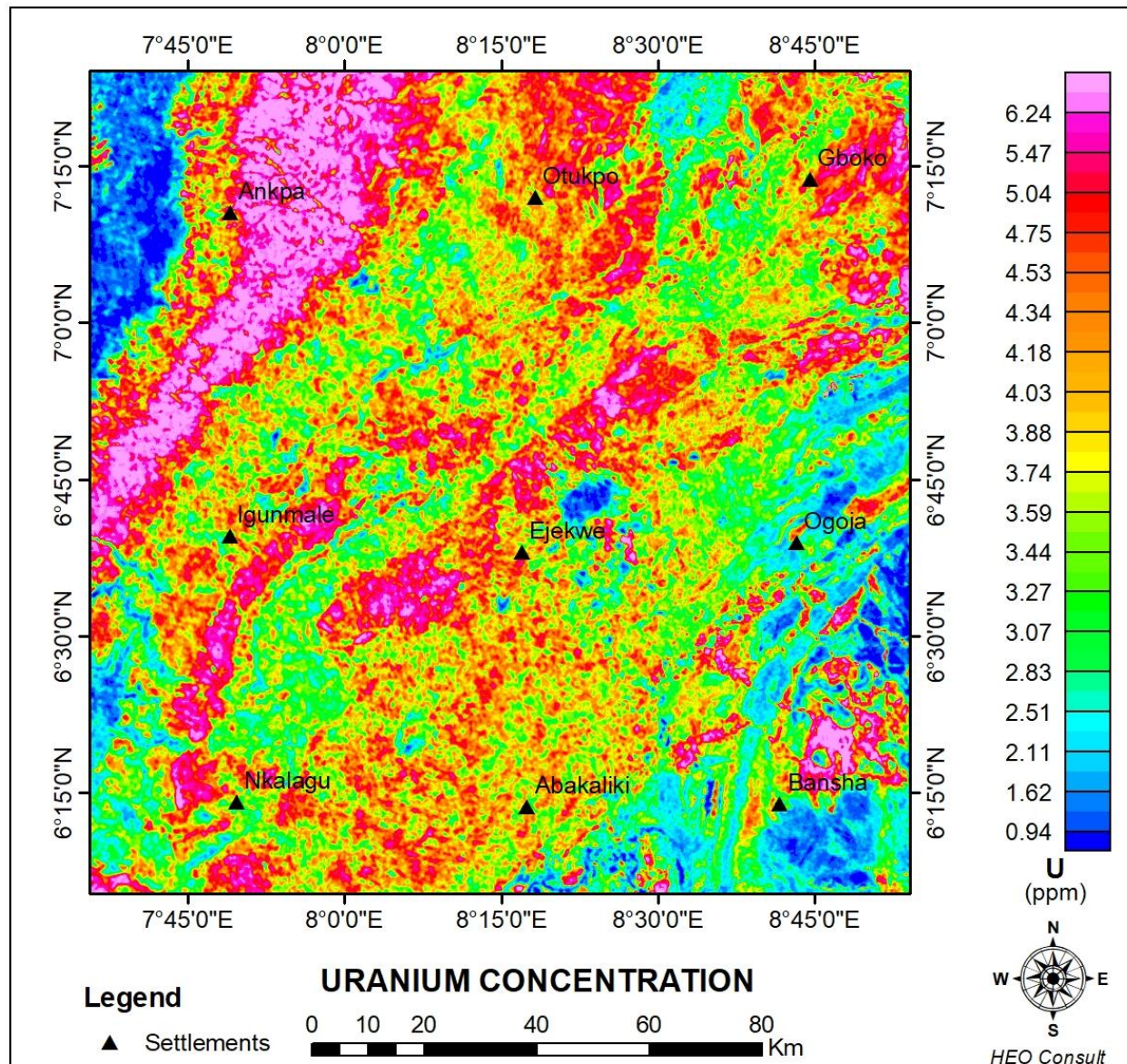


Figure 4: Equivalent uranium (eU) concentration map illustrating localized uranium enrichment and radiogenic anomalies. Elevated eU values frequently occur along fault-controlled corridors and contact zones, suggesting potential fluid-related uranium mobilization or the presence of U-bearing minerals within structurally active regions.

These do not always coincide with Th peaks, indicating uranium remobilization by hydrothermal fluids (Gobashy et al., 2024). Uranium mobility is a common indicator of active fluid pathways in mineralized systems.

Ternary Image

Red-dominant regions in the southeast reflect K enrichment; green-rich areas in the northwest represent Th-rich felsic units; blue-cyan areas indicate U enrichment (Figure 5).

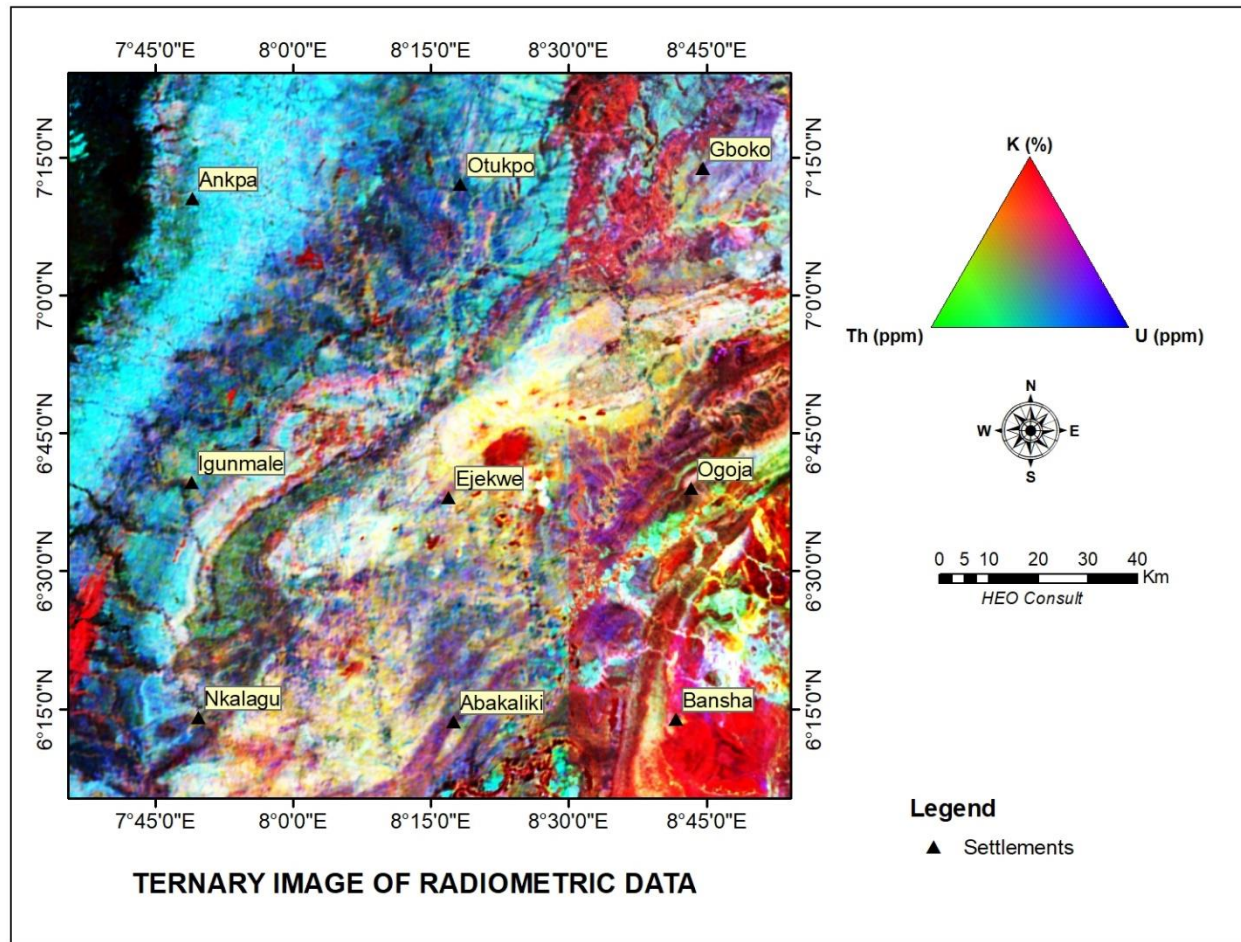


Figure 5: Ternary radioelement composite image combining K (red), eTh (green), and eU (blue). The ternary visualization enhances lithological discrimination and highlights alteration halos, felsic domains, and radiogenic anomalies. Distinct color contrasts delineate structural fabrics and lithologic boundaries with improved clarity.

Mixed colours outline transition zones and multi-element anomalies. Similar ternary patterns were used by Mamouch et al. (2022) to map alteration corridors in Morocco.

K/Th Ratio

The K/Th ranges from less than 0.004 to more than 0.097 (Figure 6). Elevated ratios (>0.04) in the central and southeastern sectors indicate potassic alteration.

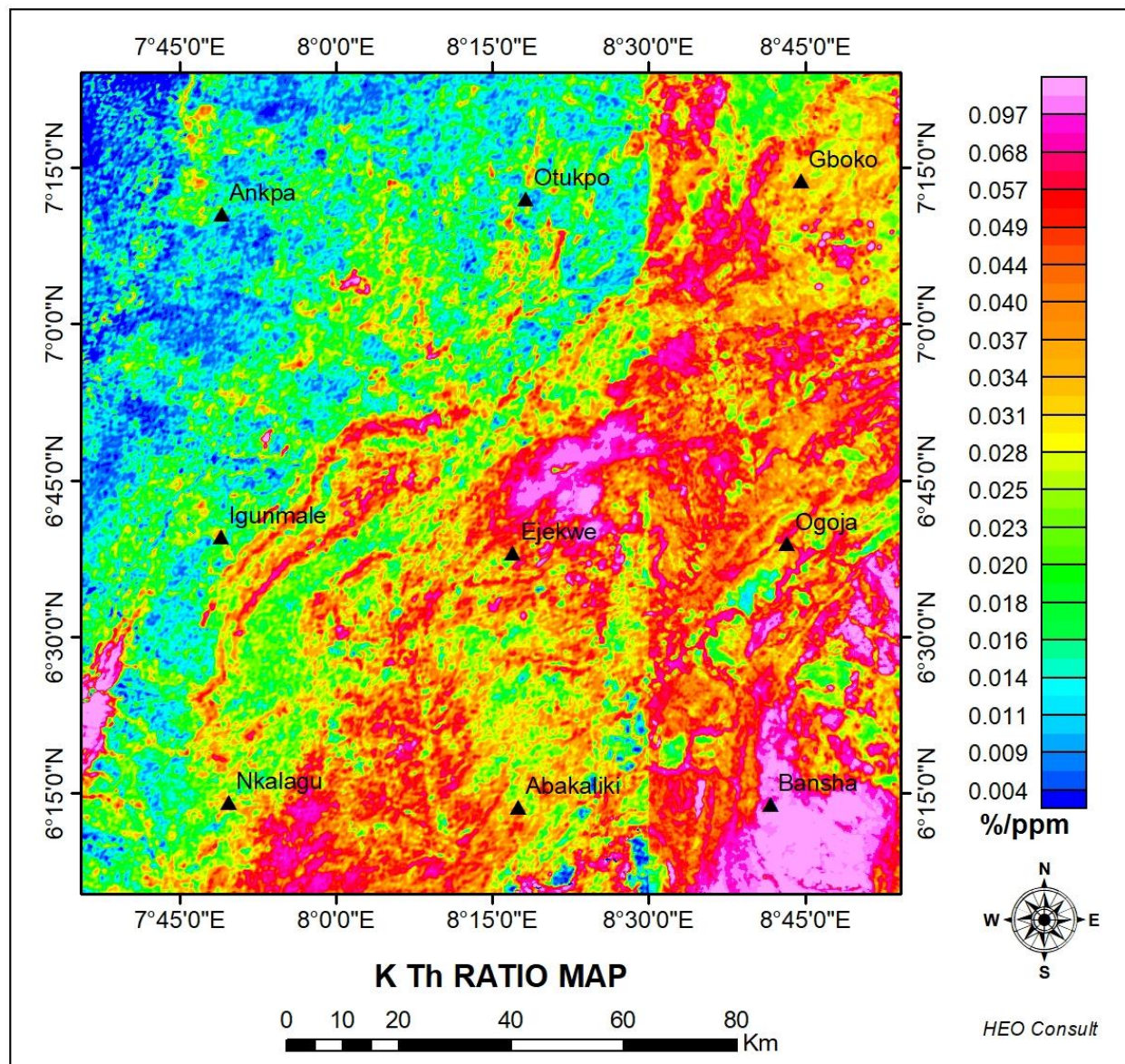


Figure 6: Potassium–thorium ratio (K/eTh) map used to emphasize zones of potassic alteration relative to thorium depletion. High K/eTh ratios delineate metasomatized corridors, hydrothermal halos, and felsic intrusive centers, providing key indicators for mineral exploration within the basement terrain.

Local anomalies exceeding 0.05 mark intense K addition along structural zones. These coincide with mapped NE–SW fabrics, consistent with Ruffell et al. (2006), who reported K/Th anomalies along structures in altered terrains.

U/Th Ratio

The U/Th values range from approximately 0.1 to more than 0.4 (Figure 7). Higher ratios (>0.3) mainly in the northwestern regions indicate uranium enrichment relative to Th.

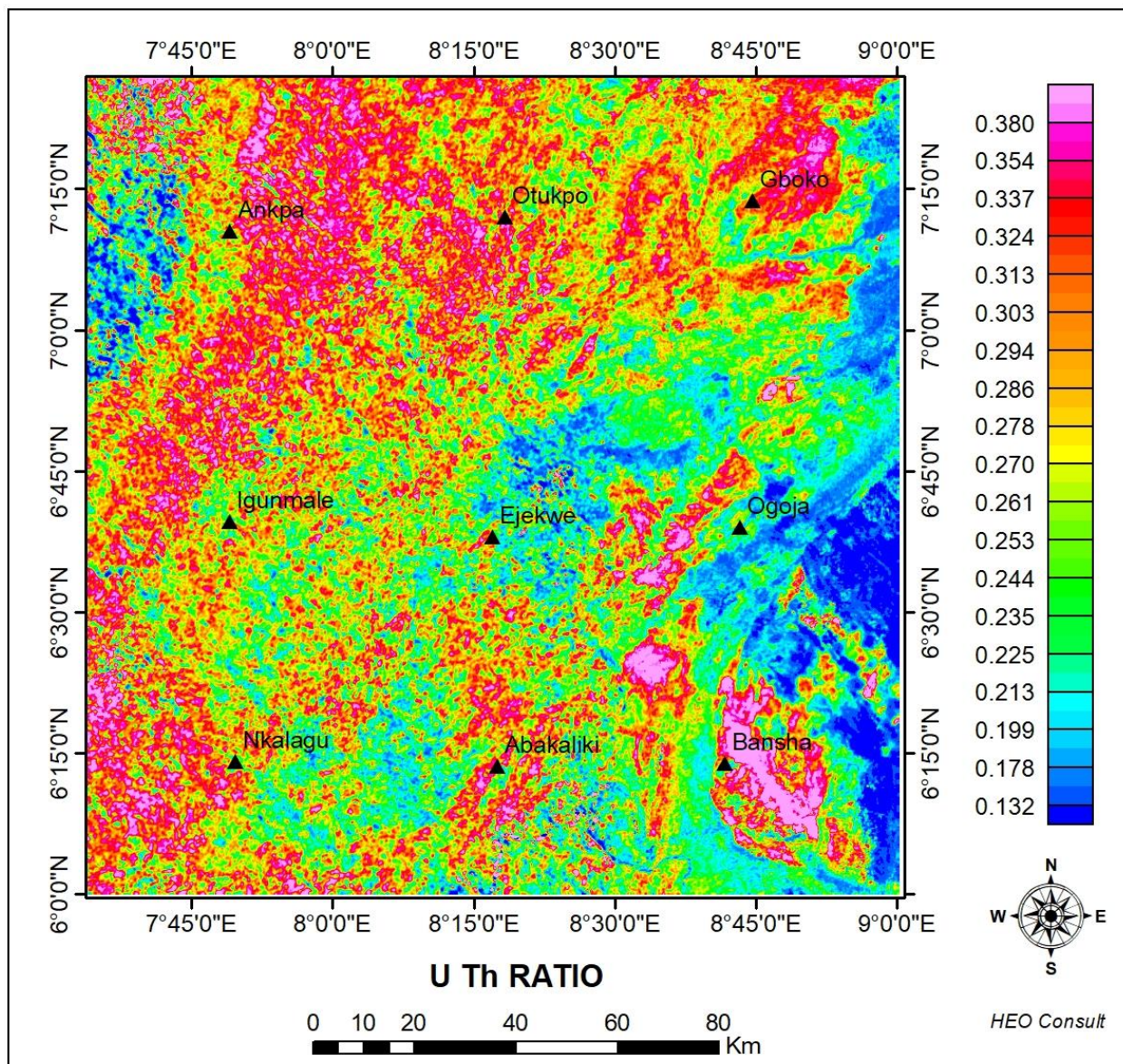


Figure 7: Uranium–thorium ratio (eU/eTh) map used to emphasize zones of uranium enrichment relative to thorium depletion.

Such patterns typically reflect hydrothermal fluid pathways (Ohwo & Soalpe, 2024). Low values (<0.2) in the southeast correspond to unaltered felsic rocks.

F-Parameter

The F-parameter ranges from below 0.007 to more than 0.2 (Figure 8).

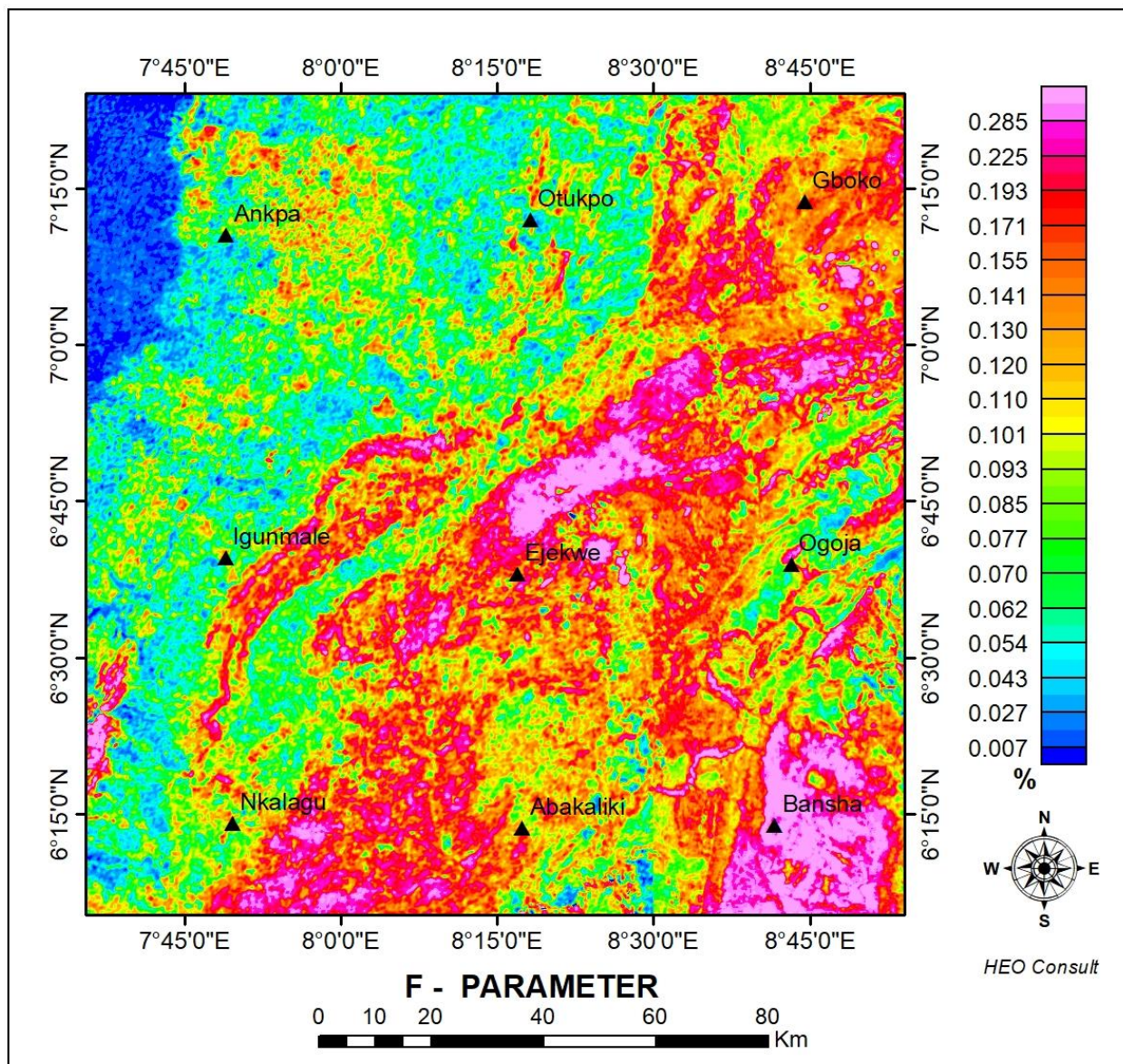


Figure 8: Efimov F-parameter map (after Efimov, 1978) illustrating regions of enhanced potassic alteration based on combined variations in K and Th. The F-parameter effectively highlights subtle alteration zones associated with hydrothermal fluid activity, offering a complementary perspective to conventional radioelement ratio analysis.

High positive values cluster in the southeastern and central areas, consistent with K addition and U mobilization accompanied by relative Th depletion. These are characteristic of hydrothermal alteration (Akinlalu, 2023; Kotb et al., 2024).

Discussion

Integrated Alteration Signatures

Several radiometric indicators consistently converge in the northwestern, central, and southeastern sectors. Potassium values exceed 1.5%, K/Th ratios are greater than 0.09, U/Th ratios exceed 0.3, and F-parameter values are greater than 0.2. This combination suggests

strong potassic alteration accompanied by uranium mobility. Such multi-parameter anomalies are widely recognized as robust indicators of hydrothermal zones, consistent with observations by Osita et al. (2025).

Lithological Discrimination

Radiometric signatures effectively distinguish felsic units, which exhibit high Th values, moderate K values, and low U/Th ratios, from mafic or intermediate rocks that have low values of all three radioelements. This behaviour aligns with results obtained by Ologe et al. (2025) in the basement complex of northwest Nigeria.

Implications for Mineralization

The southeastern and central anomalies resemble alteration systems documented in the Ife–Ilesa Schist Belt (Akinlalu, 2023), eastern Senegal (Thiam et al., 2023), and Egypt’s Eastern Desert (Kotb et al., 2024). These studies confirm that potassic alteration zones with uranium mobility are favourable targets for gold and base-metal mineralization.

CONCLUSION

Airborne radiometric interpretation has identified hydrothermal alteration zones in the study area, particularly in the southeastern and central regions, where K enrichment exceeding 1.2%, elevated K/Th and U/Th ratios, and high F-parameter values greater than 0.2 converge. These anomalies, aligned with NE–SW structural trends, mark prospective targets for orogenic gold and base-metal mineralization.

REFERENCES

Adegbuyi, O., Akinola, O. O., & Ojo, O. A. (2021). Structural controls on mineralization in the Nigerian Basement Complex: Insights from integrated geological and geophysical data. *Journal of African Earth Sciences*, 179, Article 104202. <https://doi.org/10.1016/j.jafrearsci.2021.104202>.

Akinlalu, A. A. (2023). Radiometric Mapping for the Identification of Hydrothermally Altered Zones Related to Gold Mineralization in the Ife–Ilesa Schist Belt, Southwestern Nigeria. *Indonesian Journal of Earth Sciences* (InJoES). <https://doi.org/10.52562/injoes.2023.519>.

Faruwa, A. R., Qian, W., & Obafunmilayo, O. S. (2021). Airborne magnetic and radiometric mapping for litho-structural settings and their significance for mineralization (case study). *Journal of African Earth Sciences*, 180, 104222. <https://doi.org/10.1016/j.jafrearsci.2021.104222>.

Gobashy, M. M., El-Sadek, M. A., Mekkawi, M. M., et al. (2024). Radiometric characteristics of some metallic ores and nonmetallic deposits: An example, Wadi Al-Allaqi, South Eastern Desert, Egypt. *Scientific Reports*, 14, 2443. <https://doi.org/10.1038/s41598-024-52912-9>.

Kotb, A., Gaber, G. M., Alzahrani, H., Okok, A., Elkhaliq, M. H. A., & Basheer, A. A. (2024). Unearthing Egypt’s Golden Legacy: Geophysical Insights and New Opportunities in the Central Eastern Desert. *Minerals*, 14(8), 787. <https://doi.org/10.3390/min14080787>.

Liao, G., Li, Y., Xi, Y., Lu, N., & Wu, S. (2023). Application of High-Resolution Aeromagnetic and Gamma-ray Spectrometry Surveys for Litho-Structural Mapping in Southwest China. *Minerals*, 13(11), 1424. <https://doi.org/10.3390/min13111424>.

Mamouch, Y., Attou, A., Miftah, A., Ouchchen, M., Dadi, B., Achkouch, L., Et-Tayea, Y., Allaoui, A., Boualoul, M., & Randazzo, G. (2022). Mapping of Hydrothermal Alteration Zones in the Kelāat M’Gouna Region Using Airborne Gamma-Ray Spectrometry and Remote Sensing Data: Mining Implications (Eastern Anti-Atlas, Morocco). *Applied Sciences*, 12(3), 957. <https://doi.org/10.3390/app12030957>.

Ohaebuchu, H. E., Dinneya, O. C., Nwokoma, E. U., Uzoaru, S. I., & Musa, Y. A. (2025). Unconstrained 3D Inversion of Airborne Magnetic Data for Mineral Targeting in the Southwestern Nigerian Basement Complex. *Nigerian Journal of Physics*, Volume 34(3): 3027-0936. <https://doi.org/10.62292/njp.v34i3.2025.425>.

Ologe, O., Moyi, A. M., Sanusi, F., Tsafe, U. H., & Umar, S. (2025). Interpretation of Airborne Radiometric Data of a Typical Basement Complex, Northwest Nigeria. *Arid Zone Journal of Engineering, Technology & Environment*, 21(1), 294-302. <https://www.azojete.com.ng/index.php/azojete/article/view/1032>

Osita, L. J., Mallam, A., Abdulsalam, N. N., & Nzeghi, G. J. (2025). Topographic and Radiometric Integration for Enhanced Structural Mapping in Gold Exploration: A Case Study of North Central Nigeria. *Journal of Geography, Environment and Earth Science International*, 29(11), 27-48. <https://doi.org/10.9734/jgeesi/2025/v29i11966>

Shives, R. B. K. (2000). The detection of potassic alteration by gamma-ray spectrometry: Canadian case histories. *SEG Expanded Abstracts / The Leading Edge* style record. <https://doi.org/10.1190/1.1444884>.

Thiam, A., Baratoux, D., Fall, M., Faye, G., & Ouattara, G. (2023). Multi-Parameter Statistical Analysis of K, Th, and U Concentrations in Eastern Senegal: Implications for the Interpretation of Airborne Radiometrics. *Geosciences*, 13(9), 263. <https://doi.org/10.3390/geosciences13090263>.

Xu, S., Zhang, G., Dong, G., Sun, W., Wei, D., Jin, Z., Fan, Z., Liu, Y. (2022). Radiological, geochemical and environmental assessment in Xuancheng, China: The airborne gamma-ray spectrometric view. *Journal of Geochemical Exploration*, 236, 106980. <https://doi.org/10.1016/j.gexplo.2022.106980>